Micromachines

DOI: 10.1002/anie.201201902

Acoustic Droplet Vaporization and Propulsion of Perfluorocarbon-Loaded Microbullets for Targeted Tissue Penetration and Deformation**

Daniel Kagan, Michael J. Benchimol, Jonathan C. Claussen, Erdembileg Chuluun-Erdene, Sadik Esener, and Joseph Wang**

Recent advances in micro/nanomachines have shown great promise in diverse fields.[1–13] A wide variety of chemically powered and magnetically propelled micro/nanoscale machines have been developed for specific biomedical applications ranging from lab-on-chip bioanalytical devices to site-specific drug delivery targeting. However, these micro/nanomachines lack the power and biocompatibility necessary for penetrating tissue and cellular barriers, for in vivo cargo delivery and precision nanosurgery.

Prevalent micro/nanomachine designs typically require conversion of external chemical energy, harvested from the vicinity of the machines, to promote autonomous propulsion. Several mechanisms have been developed to realize such micro/nanomachine thrust in connection to hydrogen peroxide fuel; these mechanisms include self-electrophoresis,[3,5] self-diffusiophoresis,[4] and bubble propulsion.[7,11,14] To enhance biocompatibility several groups have also explored fuel-free micro/nanomachine propulsion mechanisms, including the utilization of electrical power (i.e., diode nanowires)[15] and magnetic actuation.[16–18] Despite the inherent advantages of such externally propelled micro/nanoscale locomotion schemes, these propulsion mechanisms do not possess the thrust needed for penetrating tissue barriers and cellular membranes.[19]

Herein we present a highly efficient microscale propulsion technique that utilizes ultrasound (US) to vaporize biocompatible fuel (i.e., perfluorocarbon (PFC) emulsions) bound within the interior of a micromachine for high-velocity, bullet-like propulsion. Such remarkable micro/nanomachine thrust is sufficient for deep tissue penetration and deformation. An increase in enthalpy, which accompanies vaporization, results in energy transfer. Momentum, geometrically focused by virtue of the micromachine structure, generates projectile motion. Thus, instead of creating a device that can convert a chemical fuel, we have produced a micromachine with an on-board fuel source that is capable of releasing energy as a response to an external stimulus regardless of the surrounding environment as a response to an external stimulus.

Recently, gas and liquid PFC particles have received considerable attention owing to their biocompatible nature for intravenous injection and subsequent destruction upon ultrasound irradiation.[20,21] The decreased solubility and low diffusion coefficient of these droplets and bubbles lengthens blood circulation before an incident US wave is used to induce their destruction or cavitation.[22] PFC microbubbles or emulsions are thus extremely attractive for diverse biomedical applications, such as externally triggered site-specific drug and gene delivery capsules,[23,24] molecular imaging agents,[25,36,37] phase change contrast agents,[26,27] and blood substitutes.[27–29] However, we are unaware of earlier reports on using PFCs as an integrated fuel source for micro/nanomachine propulsion.

Similar to the externally triggered explosion experienced within a gun barrel to propel a bullet,[30] these micromachines, named herein microbullets (MB), utilize for propulsion the rapid expansion and vaporization of perfluorocarbon droplets[31] that are electrostatically bound within the machine interior and triggered by an US pulse (i.e., acoustic droplet vaporization (ADV)).[32,33] These new US-triggered, PFC-loaded microbullets can travel at remarkably high average velocities (ca. 6.3 $m s^{-1}$: over 100 times faster than the micromachines published to date)[11–14] and deeply penetrate and deform kidney tissue. The concomitance of powerful MB propulsion, biocompatible PFC emulsion fuel,[35] and deeply penetrative, yet medically safe US[34] could lead to highly targeted in vivo drug delivery, artery cleaning, gene regulation schemes, and cancer therapeutics that require higher specificity and accuracy than the current state-of-the-art.

The choice of the specific PFC compounds is also crucial as their chemical properties have a profound effect upon the efficiency of the ADV process and hence upon the resulting propulsion performance. PFC compounds with a low boiling point, such as perfluoropropane and perfluorobutane, are stable in the gaseous state and have been extensively used for the production of microbubbles for contrast-enhanced US imaging.[41] PFC compounds with a higher boiling point exist

[*] Dr. D. Kagan,[+] Dr. J. C. Claussen,[+] Dr. E. Chuluun-Erdene, Dr. S. Esener, Dr. J. Wang
Department of Nanoengineering
University of California San Diego
9500 Gilman Drive, La Jolla, CA 92093 (USA)
E-mail: sesener@ucsd.edu
josephwang@ucsd.edu
M. J. Benchimol[+]
Department of Electrical and Computer Engineering
University of California San Diego (USA)

[+] These authors contributed equally to this work.

[**] We gratefully acknowledge financial support from the National Science Foundation (Award Number CBET 0853375), National Cancer Institute (NCI-5U54A119335-05), and the National Institutes of Health (NIH R25-CA153915). The authors thank Wei Gao for help in preparing the small MBs (length ca. 8 μm).

Supporting information for this article is available on the WWW under http://dx.doi.org/10.1002/anie.201201902.

as liquids or solids, but two particular molecules, perfluoropentane (PFP; bp 29 °C at 1 atm) and perfluorohexane (PFH; bp 56 °C at 1 atm) are liquid PFC compounds that can also persist in the gaseous state—an important property for ADV.[38] Thus, in the work described herein, we distinctly functionalize micromachines with both PFH and PFP to optimize the US-triggered propulsion strategy.

A three-step fabrication strategy (Figure 1), including nanofabrication, cysteamine functionalization, and PFC emulsion binding, was utilized for preparing the US-triggered

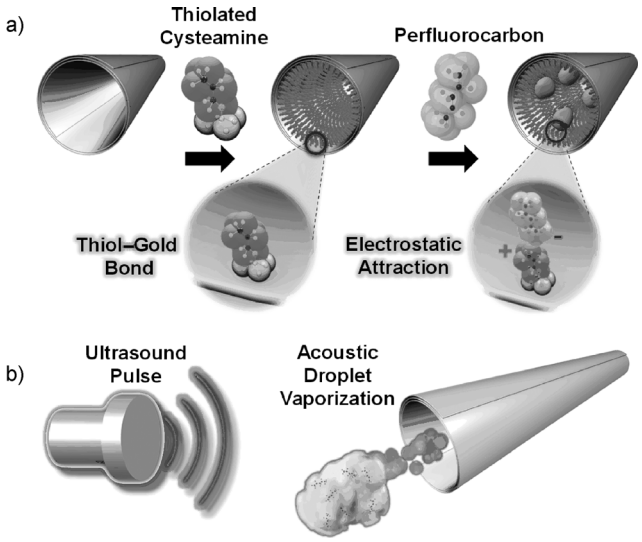

Figure 1. a) Preparation of the PFC-loaded MBs: nanofabricated MB (left), the conjugation of thiolated cysteamine to the inner Au layer of the MB (middle), electrostatic binding of the anionic PFC emulsion to the cysteamine-functionalized surface (right). Insets show magnified views of cysteamine (left) and cysteamine electrostastically bound to PFC (right). b) Schematic illustration of microbullet propulsion through acoustic droplet vaporization of the bound PFC triggered by an ultrasound pulse.

MBs. Large MBs (length ca. 40 μm, Figure 1) were created by using rolled-up thin-film nanofabrication techniques,[7,11] while for fabrication of small MBs (length ca. 8 μm) membrane-template electrodeposition was utilized (see experimental methods in the Supporting Information).[14] An embedded Ni layer facilitates magnetic washing and experimental alignment of the MBs before US pulsing to facilitate directed, linear motion during propulsion. The inner Au layer of these microtubes permits cysteamine monolayer conjugation for electrostatic attachment of PFC droplets. The slightly tapered conical structure of the MBs, owing to the angled physical vapor deposition fabrication process,[7,11] directs thrust from ADV while an embedded magnetic layer permits externally guided, magnetic alignment for precision steering.

To initiate this study, emulsion droplets of PFH (bp 56 °C),[38] were utilized because they maintain stability under physiological conditions but enable ADV upon arrival of incident US pressure waves. Moreover, the emulsion composition was designed to have efficient matching of intermolecular forces between the PFC and the surfactant; the matching of the forces is necessary to reduce interfacial tension and facilitate the conversion of nanoscale droplets. To illustrate the selective PFH-droplet immobilization strategy developed herein, fluorescently tagged PFH emulsions, stabilized by a negatively charged surfactant, were electrostatically immobilized onto the cysteamine-modified inner gold surfaces (Figure SI1 in the Supporting Information). The exposed amino group (pK_a 8.6) of the cysteamine[39] is positively charged for the prescribed experimental settings (i.e., pH range 7.4–8.0) and thus electrostatically binds to emulsions stabilized with an anionic phosphate fluorosurfactant (pK_a 7.2). Emulsions were strongly negative with a measured zeta potential of −46 mV in phosphate-buffered saline. A graphical representation of the emulsion size distribution (mean = 304.9 nm, polydispersity index = 0.144) and stability is included in the Supporting Information.

Initial US-triggered propulsion experiments reveal PFH emulsion vaporization originating from within the MBs (Figure 2a and Video 1 in the Supporting Information). A vaporized emulsion (i.e., bubble) extending out of the tail of the MB is clearly visible after the US pulsation (Figure 2a, right), thereby corroborating the assumption that formation of microscale gaseous bubbles is the result of sudden US-triggered, PFH droplet vaporization. The rapid emulsion expansion during the vaporization process (ca. 5-fold radial)[21] provides a sudden impulse that projects the MB

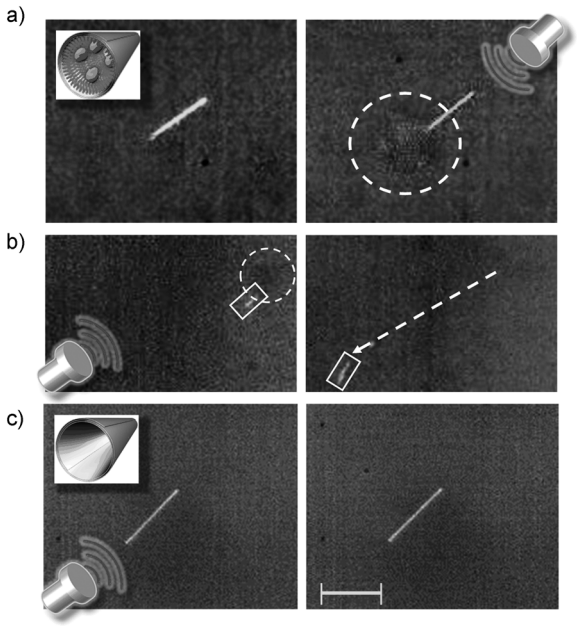

Figure 2. a) Still frame images illustrating the formation of a bubble cloud from the tail of a PFH-loaded MB upon firing of an US pulse signal. b) The trajectory (dotted arrow; right) of a PFH-loaded microbullet is imaged 55 μs after an (left) US pulse signal. A dotted circle accents the emerging vaporized PFH while boxes highlight the location of the MB. c) A MB incubated with PFH emulsion but not conjugated with cysteamine displays no emulsion expansion nor movement after a US pulse signal. Inset images show the (a) PFH-loaded MB and the (c) control MB (i.e., without cysteamine) while the US icon represents a US-triggered pulse signal (44 μs, 1.6 MPa). The images were obtained at a frame rate of 18000 frames per second (fps) using a 40X objective. Scale bar, 40 μm (a, c) and 120 μm (b).

out of the microscope field of view within an extremely short single image frame (ca. 55.6 μs). Control experiments over a longer period demonstrate that nonspecific adsorption of PFH was negligible as MBs functionalized without cysteamine (Figure 2c) or without the PFH emulsion (Video 1 in the Supporting Information) failed to produce bubbles or MB movement. US pulsations therefore have minimal effect on the locomotion of nonfunctionalized MBs.

The movement of the MBs were analyzed over a series of frames (Figure 2b obtained from Video 2 in the Supporting Information) in which the MB travels 350 μm from its initial location within 55.6 μs upon vaporization of the PFH emulsion (Figure 2b (left), dotted circle) triggered by an US pulse signal. Therefore, the MB traveled at a remarkably high average velocity of 6.3 $m s^{-1}$, which corresponds to an ultrafast relative velocity of over 158000 body lengths s^{-1}. The MB dynamics were analyzed with Stokes' law and experimental image analysis (see the Supporting Information). The initial MB velocity (56.9 s^{-1}), kinetic energy (0.764 nJ), and momentum (2.69×10^{-11} N s) were calculated with Equations (1)–(3) in conjunction with MB parameter values presented in Table SI1 in the Supporting Information (see the Supporting Information for equation derivations and parameter values):

$$v_0 = \frac{\Delta d}{\frac{m}{k}\left(1 - \frac{m}{k} e^{-\frac{kAt}{m}}\right)} \quad (1)$$

$$E_k = \frac{1}{2} m v^2 \quad (2)$$

$$p_0 = m v_0 \quad (3)$$

where k is the drag coefficient for a cylinder, m (kg) is the mass of the hollow MB , Δd (m) is the distance traveled, t (s) is time, and E_k (J) is the kinetic energy. The remarkably high initial and average MB velocities associated with US-triggered emulsion vaporization compare favorably with velocities achieved for stochastically moving microparticles propelled by water cavitation.[40]

To promote highly efficient, single-shot, and controllable MB firings, the US trigger settings (i.e., transducer pressure and pulse length) and MB fabrication (i.e., size, shape, thickness) were optimized at distinct settings. The combination of low pressure (1.6 MPa)/medium pulse length (44 μs) and high pressure (3.8 MPa)/short pulse length (4.4 μs) produced efficient linear MB locomotion from ADV without external water cavitation, while other combinatorial changes in pulse pressure and length produced water cavitation and/or sporadic MB movement (see Figures SI2,5, and 6 in the Supporting Information). Furthermore, distinctly sized MBs (40 nm thick, 40 μm long, and 2.5 μm in diameter) produced ultrafast linear motion when functionalized with PFH droplets with a diameter of 180 nm. However, MBs that were longer (lengths > 100 μm), longer and slender (60 μm long, 400 nm thick, 3 μm in diameter), and smaller MBs (8 μm long, 800 nm inner diameter) rotated uncontrollably (Figure SI3 and Video 3 in the Supporting Information), exploded (Figure SI4 and Video 4 in the Supporting Information), and stochastically agitated (Video 5 in the Supporting Information) upon US pulse firing. Additional functionalization tests revealed that lower-boiling-point emulsions (PFP, bp 29 °C)[38] vaporized more consistently at low pressures but were less stable during functionalization and increased MB explosion during US triggering. Further optimization of the emulsion size and composition could thus be used to tailor US-triggered propulsion devices for specific biomedical applications that require distinct microbullet velocity and momentum characteristics.

To demonstrate the ability to penetrate through dense materials for potential targeted delivery applications, PFH-loaded MBs were fired into tissue sections from a lamb kidney. The image sequence (Figure 3a) and Video 6 in the Supporting Information depict the deep penetration of the MB into the lamb kidney tissue section after an US pulse. These sequential images illustrate the MB before locomotion, during initial tissue penetration, and after traveling 200 μm into the tissue from a single US pulse (44 μs, 1.6 MPa). A very short US pulse (4.4 μs) at high pressure (3.8 MPa) also provided sufficient thrust for the MBs to pierce kidney tissue (Figure SI5 and Video 7 in the Supporting Information). Video 8 in the Supporting Information and Figure 3b depict the ability of the US-triggered MB to penetrate, deform, and cleave kidney tissue. Progressive images illustrate the MB capturing, deforming, and transporting a small piece of kidney tissue after an US pulse (44 μs, 1.6 MPa; Figure 3b). Thus, the US pulse pressure can be tuned to permit MB tissue piercing, deformation, or deep penetration, depending on the specifications and tissue degradation restrictions of distinct biomedical applications. Furthermore, the ability to propel multiple MBs from the same US pulse into a tissue section is displayed in Figure 3c and Video 9 in the Supporting Information. The potential power of multiple US-triggered MBs can be visualized as the MBs increase the tissue cavity area by 120% after the first US pulse (4.4 μs, 3.8 MPa) and penetrate

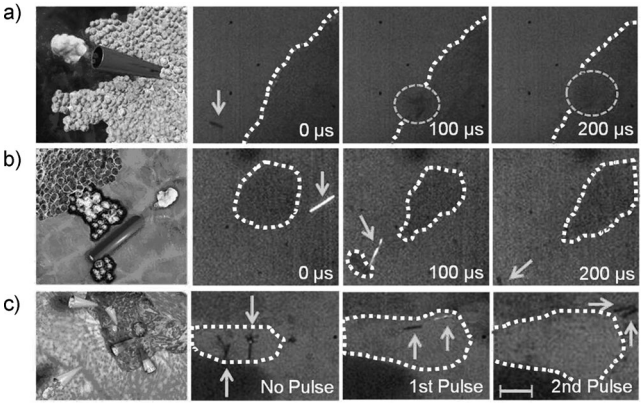

Figure 3. Computer-aided graphic (graphics on the left) and corresponding experimental images of PFH-loaded MBs a) penetrating, b) cleaving, and c) expanding a tissue following an US pulse signal. All images were taken sequentially at a frame rate of 10000 fps and 10X objective. US pulses of 44 μs/1.6 MPa were used for (a, b) and short pulses of 4.4 μs/3.8 MPa were used for (c). Dotted circles and solid arrows are used to indicate the MB's position, while curvilinear dotted lines outline the tissue. Scale bar = 100 μm in (a), 40 μm in (b), and 80 μm in (c).

the kidney tissue after a second, similarly tuned US pulse (see Figure SI6 in the Supporting Information for full image sequence).

The presented ultrasound-triggered microbullet firing technique potentially offers a safe, low-cost, and effective method to project delivery devices into dense tissue or organs. These US-triggered, PFC-loaded MBs possess the unique ability to accelerate rapidly, acquire significant momentum (2.69×10^{-11} N s), and travel at average speeds over 6 m s^{-1} (i.e., approximately 100 times faster than previous micromachines). This unprecedented MB speed and force enables lamb kidney tissue piercing, deep penetration, deformation, and cleaving—capabilities that, to our knowledge, have not been demonstrated to date with micro/nanomachines. The US-triggered MB propulsion technique is highly reproducible; approximately 80% of perfluorohexane-conjugated microbullets fire upon US pulsing, and MBs display negligible damage after multiple firing under optimized US conditions. The larger 40 μm microrockets were generally used in this study for visualization purposes, but the use of smaller 8 μm microbullets suggest that this is a scalable approach, opening the door for potential use in capillaries that are 5–10 μm in diameter. This US-triggered MB propulsion strategy should thus have a tremendous impact on diverse biomedical applications (e.g., targeted drug delivery, circulating biolistics, micro-tissue and artery-cleaning/removal schemes, precision nanosurgery, and cancer therapeutics). For example, as an alternative to treatment of bladder cancer with bacillus Calmette-Guerin (BCG), multiple US-triggered MBs could be introduced and fired into the bladder, as illustrated in Figure 3c, to create a natural inflammatory response for fighting cancer cells. While offering a similar immunoprophylactic effect, the use of these MBs may potentially eliminate harmful side effects (e.g., sepsis, dysuria, hematuria, nausea, and fever) associated with BCG.

Received: March 10, 2012
Revised: May 23, 2012
Published online: June 12, 2012

Keywords: drug delivery · electrostatic interactions · perfluorinated solvents · ultrasound · vaporization

[1] T. Mallouk, A. Sen, *Sci. Am.* **2009**, *300*, 72.
[2] G. A. Ozin, I. Manners, S. Fournier-Bidoz, A. Arsenault, *Adv. Mater.* **2005**, *17*, 3011.
[3] M. Pumera, *Nanoscale* **2010**, *2*, 1643.
[4] J. R. Howse, R. A. L. Jones, A. J. Ryan, T. Gough, R. Vafabakhsh, R. Golestanian, *Phys. Rev. Lett.* **2007**, *99*, 48102.
[5] T. R. Kline, W. F. Paxton, T. E. Mallouk, A. Sen, *Angew. Chem.* **2005**, *117*, 754; *Angew. Chem. Int. Ed.* **2005**, *44*, 744.
[6] J. Wang, *ACS Nano* **2009**, *3*, 4.
[7] Y. Mei, A. A. Solovev, S. Sanchez, O. G. Schmidt, *Chem. Soc. Rev.* **2011**, *40*, 2109.
[8] T. Mirkovic, N. S. Zacharia, G. D. Scholes, G. A. Ozin, *Small* **2010**, *6*, 159.
[9] D. Kagan, R. Laocharoensuk, M. Zimmerman, C. Clawson, S. Balasubramanian, D. Bishop, S. Sattayasamitsathit, L. Zhang, J. Wang, *Small* **2010**, *6*, 2741.
[10] S. Sanchez, A. A. Solovev, S. M. Harazim, O. G. Schmidt, *J. Am. Chem. Soc.* **2011**, *133*, 701.
[11] A. A. Solovev, Y. Mei, E. Bermudez Urena, G. Huang, O. G. Schmidt, *Small* **2009**, *5*, 1688.
[12] S. Balasubramanian, D. Kagan, C. M. Jack Hu, S. Campuzano, M. J. Lobo-Castanon, N. Lim, D. Y. Kang, M. Zimmerman, L. Zhang, J. Wang, *Angew. Chem.* **2011**, *123*, 4247; *Angew. Chem. Int. Ed.* **2011**, *50*, 4161.
[13] G. Huang, J. Wang, Y. Mei, *J. Mater. Chem.* **2012**, *22*, 6519.
[14] W. Gao, S. Sattayasamitsathit, J. Orozco, J. Wang, *J. Am. Chem. Soc.* **2011**, *133*, 11862.
[15] P. Calvo-Marzal, S. Sattayasamitsathit, S. Balasubramanian, J. R. Windmiller, C. Dao, J. Wang, *Chem. Commun.* **2010**, *46*, 1623.
[16] W. Gao, S. Sattayasamitsathit, K. M. Manesh, D. Weihs, J. Wang, *J. Am. Chem. Soc.* **2010**, *132*, 14403.
[17] A. Ghosh, P. Fischer, *Nano Lett.* **2009**, *9*, 2243.
[18] L. Zhang, J. J. Abbott, L. Dong, K. E. Peyer, B. E. Kratochvil, H. Zhang, C. Bergeles, B. J. Nelson, *Nano Lett.* **2009**, *9*, 3663.
[19] W. Gao, D. Kagan, O. S. Pak, C. Clawson, S. Campuzano, E. Chuluun-Erdene, E. Shipton, E. E. Fullerton, L. Zhang, E. Lauga, J. Wang, *Small* **2012**, *8*, 460.
[20] S. M. Bertilla, J. L. Thomas, P. Marie, M. P. Krafft, *Langmuir* **2004**, *20*, 3920.
[21] D. M. Worah, D. R. Kessler, A. R. Meuter, M. G. Huang, J.-M. Correas, S. C. Quay, *Drugs Future* **1997**, *22*, 378.
[22] I. Lentacker, S. C. De Smedt, N. N. Sanders, *Soft Matter* **2009**, *5*, 2161.
[23] S. Hernot, A. L. Klibanov, *Adv. Drug Delivery Rev.* **2008**, *60*, 1153.
[24] E. C. Unger, T. Porter, W. Culp, R. Labell, T. Matsunaga, R. Zutshi, *Adv. Drug Delivery Rev.* **2004**, *56*, 1291.
[25] E. G. Schutt, D. H. Klein, R. M. Mattrey, J. G. Riess, *Angew. Chem.* **2003**, *115*, 3336; *Angew. Chem. Int. Ed.* **2003**, *42*, 3218.
[26] N. Reznik, R. Williams, P. N. Burns, *Ultrasound Med. Biol.* **2011**, *37*, 1271.
[27] P. S. Sheeran, S. H. Luois, L. B. Mullin, T. O. Matsunaga, P. A. Dayton, *Biomaterials* **2012**, *33*, 3262.
[28] J. G. Riess, *Chem. Rev.* **2001**, *101*, 2797.
[29] G. P. Biro, P. Blais, A. L. Rosen, *Crit. Rev. Oncol. Hematol.* **1987**, *6*, 311.
[30] H. C. Park, K. T. Byun, H. Y. Kwak, *Chem. Eng. Sci.* **2005**, *60*, 1809.
[31] Z. Z. Wong, O. D. Kripfgans, A. Qamar, J. B. Fowlkes, J. L. Bull, *Soft Mater.* **2011**, *7*, 4009.
[32] O. D. Kripfgans, J. B. Fowlkes, D. L. Miller, O. P. Eldevik, P. L. Carson, *Ultrasound Med. Biol.* **2000**, *26*, 1177.
[33] A. H. Lo, O. D. Kripfgans, P. L. Carson, E. D. Rothman, J. B. Fowlkes, *IEEE Trans. Ultrason. Ferr.* **2007**, *54*, 933.
[34] S. B. Barnett, G. R. Ter Haar, M. C. Ziskin, H. D. Rott, F. A. Duck, K. Maeda, *Ultrasound Med. Biol.* **2000**, *26*, 355.
[35] C. I. Castro, J. C. Briceno, *Artif. Organs* **2010**, *34*, 622.
[36] R. Díaz-López, N. Tsapis, E. Fattal, *Pharm. Res.* **2010**, *27*, 1.
[37] R. F. Mattrey, *Am. J. Roentgenol.* **1989**, *152*, 247.
[38] T. D. Le, J. G. Weers, *J. Phys. Chem.* **1995**, *99*, 6739.
[39] S. P. Mezyk, *J. Phys. Chem.* **1995**, *99*, 13970.
[40] B. Borkent, M. Arora, C. D. Ohl, N. De Jong, M. Versluis, D. Lohse, K. A. Morch, E. Klaseboer, B. C. Khoo, *J. Fluid Mech.* **2008**, *610*, 157.
[41] A. Raisinghani, A. N. DeMaria, *Am. J. Cardiol.* **2002**, *90*, 3J.

